

Enhanced stimulated Raman scattering in slow-light photonic crystal waveguides

James F. McMillan, Xiaodong Yang, Nicolae C. Panoiu, Richard M. Osgood, and Chee Wei Wong

Optical Nanostructures Laboratory, Columbia University, New York, New York 10027

Received November 7, 2005; accepted January 18, 2006; posted February 10, 2006 (Doc. ID 65836)

We investigate for the first time, to our knowledge, the enhancement of the stimulated Raman scattering in slow-light silicon-on-insulator (SOI) photonic crystal line defect waveguides. By applying the Bloch–Floquet formalism to the guided modes in a planar photonic crystal, we develop a formalism that relates the intensity of the downshifted Stokes signal to the pump intensity and the modal group velocities. The formalism is then applied to two prospective schemes for enhanced stimulated Raman generation in slow-light photonic crystal waveguides. The results demonstrate a maximum factor of 10^4 (66,000) enhancement with respect to SOI channel waveguides. © 2006 Optical Society of America

OCIS codes: 130.2790, 290.5910, 250.5300, 230.7370.

Subwavelength silicon nanostructures such as photonic crystals and high-index-contrast photonic integrated circuits offer the opportunity to manipulate the propagation of light at subwavelength scales. Moreover, the inherent ease of integrating the silicon photonics platform with complementary metal-oxide semiconductor foundry integrated circuits offers unprecedented bandwidth per unit cost and distance in optical data communications.

Silicon, however, is at an intrinsic disadvantage for optical amplification and lasing due to its indirect bandgap and nonexistent second-order nonlinear response. Recent work has demonstrated that stimulated Raman scattering (SRS) in single-crystal silicon channel waveguides is a feasible means to achieve amplification and lasing via optical pumping.^{1–5} This is due to the intrinsically large Raman gain coefficient in silicon (being 10^3 – 10^4 times greater than for silica), and silicon nanostructures offering the benefit of high optical confinement due to the high-index contrast of silicon with air or silicon oxide. While still requiring an optical pump and possessing limited gain bandwidth, SRS can serve as an ultracompact on-chip gain medium at desired telecommunications frequencies. In order to enhance the intrinsic Raman gain of silicon, SRS in optical nanostructures exhibiting slow group velocities is currently being explored. Enhanced Raman scattering has been observed in bulk hollow-core slow-light guided-wave structures,⁶ and has also recently been suggested for photonic crystal (PhC) defect nanocavities.⁷ In addition, a semiclassical model of Raman scattering in bulk photonic crystals has been introduced.⁸ In this Letter we demonstrate theoretically for the first time the explicit enhancement of SRS in a slow-light photonic crystal waveguide (PhCWG) through a four-wave-mixing formalism from the computed modes of the line-defect waveguide. The silicon PhCWG studied here, made by removing a single row in a hexagonal lattice of holes, denoted as “W1 PhCWG,” and its projected band structure can be seen in Fig. 1. This structure supports two tightly confined modes with small group velocities, as illustrated by the two bands within the bandgap, with frequencies below the light line. The field distribution of these two modes, as computed through the plane wave expansion

method,⁹ is illustrated in Fig. 2. The strong subwavelength modal confinement of the high-index-contrast PhCWG leads to increased field intensities in the silicon gain media, permitting increased nonlinear interactions. In addition to increased field intensities from high-index confinement, there is additional SRS enhancement from the small group velocities of the PhCWG propagating modes. Physically this enhancement originates from the effective long light–matter interaction times at small group velocities. Photon localization is observed at the band edge; the photon experiences multiple scattering processes and moves very slowly through the material structure. The guided bands of a 2D PhCWG can be designed to be as flat as desired ($v_g \equiv d\omega/dk$) for slow-light behavior, and group velocities as low as $10^{-2}c$ – $10^{-3}c$ have been demonstrated.^{10,11}

In SRS for silicon, an incident photon interacts with the LO and TO phonons. The strongest Stokes peak arises from the single first-order Raman phonon at the center of the Brillouin zone. The generation of the Stokes photons can be understood classically as a third-order nonlinear effect; this formalism has been used to model SRS in silicon-on-insulator (SOI) waveguides, both in cw¹² and pulsed¹³ operations. It can be modeled in bulk materials as a degenerate

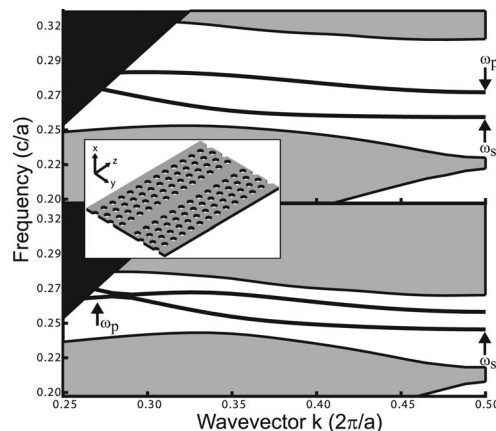


Fig. 1. Projected band structure of silicon W1 PhCWG indicating pump and Stokes frequencies. Top, scheme 1, $r/a = 0.29$. Bottom, scheme 2, $r/a = 0.22$, $h/a = 0.6$ in both cases. Inset, W1 PhCWG.

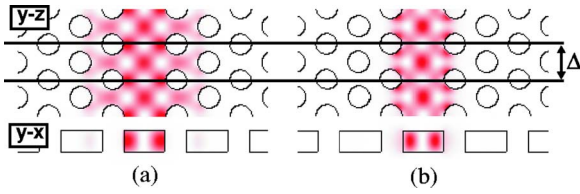


Fig. 2. Calculated bound states of a hexagonal lattice W1 PhCWG with defect modes separated by the LO–TO optical phonon (scheme 1). (a) Stokes. (b) Pump.

four-wave-mixing problem involving the pump and Stokes beams. The important material parameter is the third-order nonlinear Raman susceptibility, χ^R . For silicon, at resonance, χ^R is defined by the components $\chi_{ijij}^R = -i\chi^R = -i11.2 \times 10^{-18} \text{ m}^2 \text{ V}^{-2}$ ($i, j = 1, 2, 3$).¹² An additional symmetry, imposed by the crystal point group ($m\bar{3}m$ for Si), is $\chi_{iijj}^R = 0.5\chi_{ijij}^R$.¹⁴ These components and their permutations as defined by the crystal point group define the SRS in a silicon crystal. For our purpose we shall consider scattering in silicon along the $[1\bar{1}0]$ direction since practical devices are fabricated along this direction due to the favorable cleaving of silicon along this direction.

For bulk silicon, the evolution of the Stokes beam is defined by the following equation:

$$\frac{dI_s}{dz} = -\frac{3\omega_s \text{Im}(\chi_{\text{eff}}^R)}{\varepsilon_0 c^2 n_p n_s} I_p I_s, \quad (1)$$

where $\chi_{\text{eff}}^R = \sum_{ijkl} \chi_{ijkl}^R \hat{\alpha}_i \hat{\beta}_j \hat{\beta}_k \hat{\alpha}_l$. Here $\hat{\alpha}$ and $\hat{\beta}$ are unit vectors along the polarization directions of the pump and Stokes beams, respectively. Equation (1) describes the gain of the Stokes intensity, I_s . It shows an intrinsic dependence on the polarization and the phonon selection rules through χ^R , and the intensity of the pump beam by I_p . The bulk solution also describes SRS in dielectric waveguides, where χ_{eff}^R is averaged over the waveguide mode field distribution.

A PhCWG presents a very different field distribution from the bulk or dielectric waveguide case. As shown in the computed modal profiles of Fig. 2, the mode differs from that of a conventional channel waveguide in that it exhibits a periodic variation in the direction of propagation. We introduce the modal distribution of the pump and Stokes modes in a Bloch–Floquet formalism,

$$\mathcal{E}_{n,\mathbf{k}_n}(\mathbf{r}, \omega_n) = \mathbf{E}_{n,\mathbf{k}_n}(\mathbf{r}, \omega_n) \exp[i\mathbf{k}(\omega_n) \cdot \mathbf{r}], \quad (2)$$

where n is a mode index ($n=p, s$), $\mathbf{k}_n = \mathbf{k}(\omega_n)$ is the mode wave vector, $\mathbf{E}_{n,\mathbf{k}_n}(\mathbf{r}, \omega_n)$ is the modal distribution within a unit cell of the PhC, defined in Fig. 2, and obeys the Bloch boundary condition $\mathbf{E}_{n,\mathbf{k}_n}(\mathbf{r} + \Delta, \omega_n) = \mathbf{E}_{n,\mathbf{k}_n}(\mathbf{r}, \omega_n)$. Δ defines the length of the unit cell in the direction of propagation; for a W1 waveguide this equals the PhC lattice constant a . To develop the evolution, we employ the Lorentz reciprocity theorem,^{13,15}

$$\begin{aligned} & \frac{\partial}{\partial z} \int_A [\mathbf{E}_{n,\mathbf{k}_n}^* \times \tilde{\mathbf{H}} + \tilde{\mathbf{E}} \times \mathbf{H}_{n,\mathbf{k}_n}^*] \cdot \hat{\mathbf{e}}_z dA \\ & = i\omega \int_A \mathbf{P}^R \cdot \mathbf{E}_{n,\mathbf{k}_n} dA. \end{aligned} \quad (3)$$

This relates the unperturbed linear PhCWG modes of the pump or Stokes wavelengths, $\{\mathbf{E}_{n,\mathbf{k}_n}, \mathbf{H}_{n,\mathbf{k}_n}\}$, to those of the nonlinearly induced fields, $\{\tilde{\mathbf{E}}, \tilde{\mathbf{H}}\}$. The envelopes of the fields are defined as

$$\tilde{\mathbf{E}}(\mathbf{r}) = u_s(z) \mathbf{E}_{s,\mathbf{k}_s}(\mathbf{r}, \omega_s) + u_p(z) \mathbf{E}_{p,\mathbf{k}_p}(\mathbf{r}, \omega_p), \quad (4a)$$

$$\tilde{\mathbf{H}}(\mathbf{r}) = u_s(z) \mathbf{H}_{s,\mathbf{k}_s}(\mathbf{r}, \omega_s) + u_p(z) \mathbf{H}_{p,\mathbf{k}_p}(\mathbf{r}, \omega_p), \quad (4b)$$

with the assumption that the change in the pump and Stokes field amplitudes, $u_p(z)$ and $u_s(z)$, respectively, over the length of the unit cell of the waveguide is very small [$\Delta(du_{p,s}/dz) \ll 1$]. Taking the fields as defined in Eq. (4) and substituting into Eq. (3), we derive the dependence of the Stokes amplitude on the longitudinal distance, z ,

$$\frac{du_s(z)}{dz} = \frac{i\omega_s}{4P_s \Delta} \int_{V_0} \mathbf{P}^R(\mathbf{r}, \omega_s) \cdot \mathbf{E}_{s,\mathbf{k}_s}(\mathbf{r}, \omega_s) dV, \quad (5)$$

where P_s is the mode power and $\mathbf{P}^R(\mathbf{r}, \omega_s) = 6\varepsilon_0 \hat{\chi}^R : \mathbf{E}_{p,\mathbf{k}_p}^*(\mathbf{r}) \mathbf{E}_{p,\mathbf{k}_p}(\mathbf{r}) \mathbf{E}_{s,\mathbf{k}_s}(\mathbf{r}) |u_p|^2 u_s$. The integral in Eq. (5) is taken over the volume (V_0) of the unit cell of the mode. Furthermore, the group velocity is expressed by the following equation¹⁵:

$$v_g^{p,s} = \frac{P_{p,s} \Delta}{\frac{1}{2} \varepsilon_0 \int_{V_0} \varepsilon(\mathbf{r}) |\mathbf{E}_{p,s}(\mathbf{r}, \omega_{p,s})|^2 dV}. \quad (6)$$

With Eqs. (4) and (6), and by rewriting Eq. (5) in terms of the intensity, an equation for the intensity of the Stokes mode inside the PhCWG is obtained,

$$\frac{dI_s}{dz} = -\frac{3\omega_s}{\varepsilon_0 v_g^p v_g^s} \kappa I_p I_s, \quad (7)$$

where

$$\kappa = \frac{\Delta A_{\text{eff}} \text{Im} \left[\int_{V_0} \mathbf{E}^*(\omega_s) \cdot \hat{\chi}^R : \mathbf{E}^*(\omega_p) \mathbf{E}(\omega_p) \mathbf{E}(\omega_s) dV \right]}{\left[\frac{1}{2} \int_{V_0} \varepsilon(\mathbf{r}) |\mathbf{E}(\omega_p)|^2 dV \right] \left[\frac{1}{2} \int_{V_0} \varepsilon(\mathbf{r}) |\mathbf{E}(\omega_s)|^2 dV \right]} \quad (8)$$

is the effective susceptibility. Here, the effective area A_{eff} is defined as the average modal area across the volume V_0 ,

$$A_{\text{eff}}^2 = \frac{\left(\int_{V_0} x^2 |\mathbf{E}(\omega_s)|^2 dV \right) \left(\int_{V_0} y^2 |\mathbf{E}(\omega_s)|^2 dV \right)}{\left(\int_{V_0} |\mathbf{E}(\omega_s)|^2 dV \right)^2}. \quad (9)$$

The final equation, Eq. (7), shows the explicit inverse dependence the Stokes mode amplification has on the group velocities of the pump and Stokes modes. When compared to Eq. (1), which shows an inverse dependence on c^2 , it can be seen that equivalent Raman gains at lower pump powers (I_p) can be achieved in a PhCWG at frequencies with low group velocities.

Table 1 shows the results of Eq. (7) as being applied to two different PhCWG schemes for SRS. The group velocities are calculated from the slope of the projected band structure. The first (scheme 1) involves utilizing both the guided modes of the W1 waveguide; odd parity is the pump mode and even parity is the Stokes mode. The wavelength separation of the modes at the edge of the Brillouin zone is matched to the LO-TO frequency separation of the pump and Stokes beams [15.6 THz in Si (Ref. 16)]. The second (scheme 2) utilizes a wide bandwidth PhCWG¹⁷ for the Stokes and pump modes to exist both in the fundamental mode and below the light line. The arrows in Fig. 2 indicate the pump and Stokes frequency locations for both schemes.

From the results of Table 1, the Raman gain, which is proportional to $\kappa/v_g^p v_g^s$, is enhanced by up to approximately 10^4 (scheme 1, 66 000; scheme 2, 86) times compared to bulk Si based on a comparison of the respective group velocities. The results in Table 1 also show a κ value of the same order with a conventional SOI waveguide.¹³ In addition, we note a reduction in κ in scheme 1 as compared to scheme 2, due to the lower modal overlap. However, the single mode (scheme 2) operation has the disadvantage that only the Stokes mode, is at low group velocities for enhanced SRS.

The above results highlight the benefits of SRS enhancement through slow-light interactions in compact PhCWG schemes. This approach can be readily extended to include two photon and bulk free carrier absorption effects¹³ by the addition of loss terms to Eq. (7), which may limit the effective Raman gain in PhCWGs. These effects, in the experimental realization of silicon SRS amplification and lasing in slow-light PhCWGs, can be surmounted with pulsed-laser operation⁴ or p-i-n diodes⁵ to sweep the free carriers.

In addition, we note recent theoretical¹⁸ and experimental¹⁹ studies of PhCWGs, which show that slow group velocity modes exhibit increased scattering losses. These losses are from coupling and intrinsic

(backscatter) reflection. Coupling into slow-light modes is currently the dominant loss experimentally, although this can in principle be reduced through careful adiabatic coupling between the PhCWGs and input-output channel bus waveguides. Moreover, with thorough attention to fabrication disorder, reflection losses in PhCWG are suggested to be comparable with index-guided waveguides.²⁰ These scattering losses can thus potentially be smaller than the enhanced SRS gain discussed, permitting the possibility for compact silicon Raman amplifiers and lasers. We also note that, for the same desired Raman gain, the device length is reduced by $(c/v_g)^2$, allowing compact integration for high-density photonic circuits.

This research was sponsored in part by DARPA, and the Columbia Initiatives in Science and Engineering in Nanophotonics. N. C. Panoiu and R. M. Osgood acknowledge financial support from AFOSR through contracts FA95500510428 and FA9550-04-C-0022; and through the NSF, grant ECS-0523386. The authors also thank Steven G. Johnson for useful discussions on the low group velocity scattering. C. W. Wong's e-mail address is cww2104@columbia.edu.

References

1. R. L. Espinola, J. I. Dadap, R. M. Osgood, S. J. McNab, and Y. A. Vlasov, *Opt. Express* **12**, 3713 (2004).
2. T. K. Liang and H. K. Tsang, *Appl. Phys. Lett.* **85**, 3343 (2004).
3. Q. Xu, V. R. Almeida, and M. Lipson, *Opt. Express* **12**, 4437 (2004).
4. O. Boyraz and B. Jalali, *Opt. Express* **12**, 5269 (2004).
5. H. S. Rong, A. S. Liu, R. Jones, O. Cohen, D. Hak, R. Nicolaescu, A. Fang, and M. Paniccia, *Nature* **433**, 292 (2005).
6. S. O. Konorov, D. A. Akimov, A. N. Naumov, A. B. Fedotov, R. B. Miles, J. W. Haus, and A. M. Zheltikov, *JETP Lett.* **75**, 66 (2002).
7. X. Yang and C. W. Wong, *Opt. Express* **13**, 4723 (2005).
8. L. Florescu and X. Zhang, *Phys. Rev. E* **72**, 016611 (2005).
9. S. G. Johnson and J. D. Joannopoulos, *Opt. Express* **8**, 173 (2001).
10. M. Notomi, K. Yamada, A. Shinya, J. Takahashi, C. Takahashi, and I. Yokohama, *Phys. Rev. Lett.* **87**, 253902 (2001).
11. H. Gersen, T. J. Karle, R. J. P. Engelen, W. Bogaerts, J. P. Korterik, N. F. van Hulst, T. F. Krauss, and L. Kuipers, *Phys. Rev. Lett.* **94**, 073903 (2005).
12. B. Jalali, R. Claps, D. Dimitropoulos, and V. Raghunathan, *Top. Appl. Phys.* **94**, 199 (2004).
13. X. Chen, N. C. Panoiu, and R. M. Osgood, *IEEE J. Quantum Electron.* **42**, 160 (2006).
14. R. Loudon, *Adv. Phys.* **13**, 423 (1964).
15. A. W. Snyder and J. D. Love, *Optical Waveguide Theory* (Chapman-Hall, 1983).
16. P. A. Temple and C. E. Hathaway, *Phys. Rev. B* **7**, 3685 (1973).
17. E. Dulkeith, S. J. McNab, and Y. A. Vlasov, *Phys. Rev. B* **72**, 115102 (2005).
18. S. Hughes, L. Ramunno, J. F. Young, and J. E. Sipe, *Phys. Rev. Lett.* **94**, 033903 (2005).
19. Y. A. Vlasov and S. J. McNab, *Opt. Lett.* **31**, 50 (2006).
20. M. L. Povinelli, S. G. Johnson, E. Lidorikis, J. D. Joannopoulos, and M. Soljačić, *Appl. Phys. Lett.* **84**, 3639 (2004).

Table 1. Group Velocity and Effective Susceptibility in PhCWG Schemes

Scheme	v_g^s	v_g^p	$\kappa (\times 10^{-19} \text{ m}^2 \text{ V}^{-2})$
1	0.00017c	0.0077c	0.55
2	0.0041c	0.24c	2.02